J. Min. Metall. Sect. B-Metall. 54 (2) B (2018) 169 - 177

Journal of Mining and Metallurgy,
Section B: Metallurgy

# MICROSTRUCTURE CHARACTERIZATION AND QUANTITATIVE ANALYSIS OF COPPER ALLOY MATRIX COMPOSITES REINFORCED WITH WC-*x*Ni POWDERS PREPARED BY SPONTANEOUS INFILTRATION

**I. Daoud [a], Dj. Miroud [a], R. Yamanoglu [b*]**

[a] University of Sciences and Technology HOUARI BOUMEDIENE, Laboratory of Science and Materials Engineering, Algeria
[b] Kocaeli University, Department of Metallurgical and Materials Engineering, Izmit, Turkey

*(Received 25 December 2017; accepted 30 March 2018)*

***Abstract***

*In this study, copper alloy matrix composites reinforced with tungsten carbide (WC) particles with the addition of different Ni contents (0, 3, 5, 7, and 10 wt.%) were prepared by the spontaneous infiltration process. Image analysis was used to quantify the microstructural parameters, such as the particle size and distribution, area fraction, binder mean free path, and pore size. The effect of Ni addition on the microstructure, density and hardness are discussed. The results show that a small addition of Ni improves the densification of the infiltrated composites. The highest density value of 11.84 g/cm$^3$ with a hardness of 327 HV was obtained for the infiltrated composite with the addition of 3 wt.% of Ni. The quantitative analysis results are in good agreement with the microstructure properties and hardness results.*

***Keywords:*** *Metal matrix composite; WC particles; Image analysis; Quantification; Microstructure*

## 1. Introduction

Metal matrix composites (MMCs) are multi-phase materials that combine the properties of both their original components, consisting of metal as the matrix phase and particles or fibers as the reinforcement phase. This combination aims to enhance the final properties of the composites, which cannot be achieved when these components are used independently. The large variety available for the matrix and the reinforcements has made these composites indispensable in a wide range of sectors, including the automotive, petroleum, oil and gas industries [1-8]. As such, copper or copper alloy matrix composites reinforced with ceramic particles are an attractive metal matrix composite combination. These composites display excellent properties with high strength and wear resistance originating from the reinforcement phase. In addition they present high fracture toughness, emanating from the matrix phase. Copper or copper alloy matrix composites have received particular interest for structural applications, notably in wear applications, such as cutting, drilling, and mining tools [7-9], electrical contact applications [10, 11] and coatings [12]. In particular, copper alloys reinforced with WC particles composites are extensively used as the solid body of drilling bits in the gas, oil and petroleum industries [7, 9].

Bits are usually produced by the hot press sintering [13-17] or the melt infiltration [9, 18-21]. As an attractive process to produce these MMCs, the spontaneous infiltration process enables the possibility of realizing complex shapes with a near-net-shape in one step, eliminating all the additional process, such as machining or grinding operations [22-24]. During the spontaneous infiltration process, a molten metal is drawn under capillary forces and filled into the connected pore system of a reinforcing skeleton, followed by a rearrangement of the physical contact of the component interface. Finally, component interactions take place for good interfacial bonding between the matrix and reinforcement particles [22, 23, 25]. The conditions that induce infiltration depend mainly on wettability, capillary forces and the reaction between the phases of the composite [22-26]. The major problem with the spontaneous infiltration process is that molten metals do not generally wet ceramic particles. Moreover, copper presents poor wettability on WC [22, 27]. However, some copper alloys present good wettability on WC particles. Furthermore, alloying elements (e.g., Ni, Ti, Al, and Co) can also enhance the wettability between the matrix and the reinforcement. De Maced et al. investigated the wetting and spreading effect of nickel on WC particles [28]. They found that the spreading of Ni on the WC interface during solid-state sintering provided a higher wettability and the enhanced densification behavior.

*Corresponding author: ryamanoglu@gmail.com

DOI:10.2298/JMMB171225005D

In addition, Ni has been reported as a good wetting binder on WC particles for composites [29-33].

Alternatively, with technological progress, the need for the development of new materials with high performances requires the investigation of the relationship between the microstructure and the final properties. With the aim of understanding this relationship, extensive research through the development and use of various methods of microstructure quantification, such as image analysis [34-36], has been carried out. Recently, the image analysis technique has found a wide range of interest in materials science and engineering [34, 37, 38]. This technique can be applied to perform quantitative characterization and statistical presentation of material microstructures to provide useful information regarding microstructure features. The exploration of microstructure behavior through image analysis allows the control and optimization of the final properties and performance of a material. Several studies have been performed with the use of image analysis in the quantification of the microstructure parameters to understand their effect on the properties of sintered materials and composites [39-43]. Shen et al. [39] studied the evolution of local microstructure features to evaluate the densification and distortion behavior during initial stage liquid phase sintering at an effective sintering time using the image analysis technique. Petersson et al. [40] investigated the densification behavior of a WC-Co material at an early stage of sintering to obtain pore size distributions using the image analysis technique.

In the current study, copper alloy matrix composites reinforced with WC particles with the addition of different Ni contents (0, 3, 5, 7, and 10 wt.%) were prepared by the spontaneous infiltration process. The microstructure of the infiltrated composites was analyzed with the image analysis technique in order to quantify the different microstructure parameters, such particle size and distribution, the area fraction of the reinforcement phase, the binder mean free path and pore size. Density and hardness were also investigated. The purpose of this work is to study and analyze the microstructural feature evolution of the infiltrated composites with the addition of Ni. These results are used to create a relationship between the microstructure and composite composition.

## 2. Experimental

WC (99.7% purity, average particle size of 80 μm) and nickel (99.7% purity, average particle size of < 50 μm) were used in this study. A copper-based alloy consisting of 30 wt.% manganese and 1 wt.% phosphorus was used as a binder. The WC-*x*Ni (x = 0, 3, 5, 7, and 10 wt.%) powders were mixed in a turbula mixer for 2 h. The mixed powders were filled into a graphite mold to obtain similar composites with 10 mm height and 14 mm diameter. The binder was placed as lumps on the top of the powders. A Borax flux was also loaded on top of the binder to purify the molten matrix. The infiltration process was performed under $H_2$ atmosphere, with a heating and cooling rate of 5°C/min at 1050°C as an infiltration temperature, and for 30 min as the holding time. The infiltrated composites were cooled to room temperature inside the furnace under $H_2$ atmosphere. The densities of the infiltrated composites were measured by the Archimedes' method according to ASTM Standard B962-08 [44]. For microstructural quantification using the image analysis technique, the composites were cut vertically in the direction of infiltration and then cold mounted. The composites were prepared using silicon carbide papers from 180 to 1200 grit and then polished with 9, 6, 3, and 1 μm diamond solution. The Vickers hardness of the composites was measured with an indentation load of 30 kgf and a dwelling time of 10 s [45], with ten tests performed and the average values were given.

Microstructural quantifications, including particle size, porosity, area fraction and binder mean free path, were collected using different micrographs taken by optical and scanning electron microscopy (SEM) from the infiltrated composites at various positions from each sample (top, middle and bottom). Free software "ImageJ" was used for the image analysis process. This software is created by the National Institute of Health (https://imagej.nih.gov/ij/), USA. The image analysis technique is based on a color threshold method to separate the particles, binder and pores. For each microstructure parameter, the software passes through the step of thresholding to transform the color image to binary mode. There is a need for some corrections using image processing in some steps to eliminate image defaults. In some case, the software is selected to recognize all particles boundaries and some of the hidden or over-segmented particle boundaries need a manual correction. The porosity and pore size were calculated from the polished samples using optical images. For each sample, ~30 micrographs (100X) from the three layers of composites were used. The pore size measurements were combined for data analysis. The pore size was assimilated as the diameter of the equivalent area of the pore, and the porosity was calculated as the percentage of the area fraction of all the pores. Since the image analysis is based on the color threshold to discriminate between the pores and the other microstructure components, it was difficult to differentiate between the pores and the artifacts or the over-segmented particle boundaries. For this reason, the measured objects with a 0.5 $\mu m^2$ area or less were eliminated from the pore size and porosity analysis.

The particle size of the WC particles was calculated from the equivalent area of each particle using SEM micrographs (100X) from the top, middle and bottom of each composite. A macro was written with the software ImageJ to calculate the particle size and the area fraction simultaneously. The binder mean free path was calculated as the average distance between the WC particles in both the horizontal and vertical directions. A grid was used on the binary image to calculate this distance.

## 3. Results and discussion

### *3.1 Microstructural characterization*

For composite materials prepared by the liquid phase route, the microstructure quality is an important parameter. The most important features of the composite microstructures are the distribution of reinforcing particles, matrix properties, bonding strength of the interface between matrix and reinforcement particles, and porosity characteristics. Figure 1 shows typical SEM micrographs of the infiltrated composites with varying Ni content (0 and 3 wt.%). The microstructure reveals a uniform distribution of the WC particles within the matrix phase and no agglomerate or cluster of WC particles was observed in the microstructure of all composites.

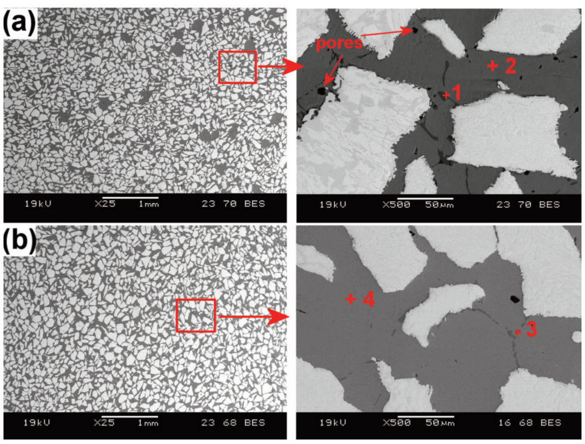


***Figure 1**. SEM micrographs of the infiltrated copper alloy matrix composites reinforced with (a) WC and (b) WC-3Ni*

***Table 1.** The chemical composition of the different phases presented in the matrix measured by ESD (Figure 1)*

| Regions | Composition (wt. %) | | | |
|---|---|---|---|---|
| | Cu | Mn | P | Ni |
| -1 | 4.35 | 70.33 | 25.32 | - |
| -2 | 70.28 | 29.27 | 0.45 | - |
| -3 | 2.37 | 69.14 | 24.62 | 3.87 |
| -4 | 67.43 | 28.17 | 0.31 | 4.1 |

No de-bonding or fracture defaults at the matrix/reinforcement interface were observed, indicating the good wetting of the reinforcement particles by the molten matrix. All the WC particles are well engulfed by the matrix. The microstructure of the infiltrated composites is mainly composed of two phases: (i) the reinforcement phase presented by WC particles with a bright contrast, and (ii) the matrix phase (copper alloy) with a greycontrast. Besides, the matrix phase exhibits the presence of an interdendritic spacing with dark contrast (Figure 1, regions (1) and (3)). The EDS analysis of the different phases present in the matrix are given in Table 1. The EDS analysis shows that the matrix phase for the composites without Ni addition (Figure 1, region (2)) is composed of a Cu-Mn solid solution (s.s), with low P content. While, it contains Cu, Mn, and Ni for the composites with Ni addition. However, the interdendritic spacing is mainly enriched with Mn and P for composites without Ni addition. While it contains Mn, P, and Ni for the composites with the addition of Ni. Both of these interdendritic spacing contain a small amount of copper. Moreover, it can be seen that the microstructure of composite reinforced with WC particles without Ni addition (see Figure 1(a)) exhibits the presence of more evenly spaced WC particles in the matrix. However, with the addition of Ni (see Figure 1(b)), more obvious and closely-packed WC particles can be observed. The presence of pores in the matrix phase is also observed.

Figure 2 presents high magnification micrographs and their EDS analysis of the different elements (W, Cu, Mn, and Ni) at the WC particles/matrix interface of the composites with the addition of 0, 3 and 7 wt.% Ni. Due to the low concentration of P, their elemental analysis was not added. The EDS analysis shows sharp curves at WC particles/matrix interface for all the composites. The concentration of WC was negligible in the matrix. In addition, no diffusion is observed of matrix elements (Cu, Mn, and Ni) into the WC particles, which indicates that the WC particles/matrix is clean. Prior work showed that the solubility of the WC particles is limited in copper or copper alloys [12, 46, 47]. Thus the WC particles retained their initial shape and surface morphology. Liu et al. [12] reported similar results for a copper alloy reinforced with WC particles prepared with centrifugal infiltration.

### *3.2 Density*

The density results of the infiltrated composites as a function of Ni content are shown in Figure 3. It can be found that the density increases with the addition of 3 wt.% of Ni, and then it decreases with the increase of Ni content. This increase in density can be attributed to the role of Ni in enhancing the wettability

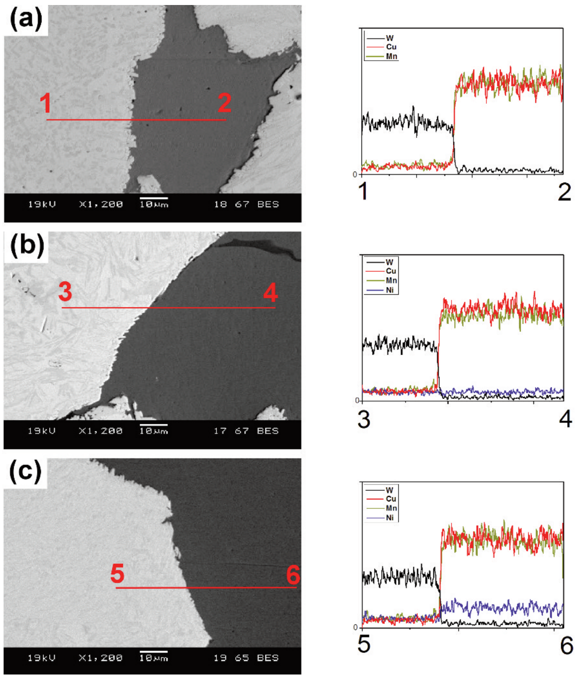


*Figure 2*. *SEM micrographs and their EDS analysis at the WC particles/matrix interfaces of the infiltrated copper alloy matrix composites reinforced with (a) WC, (b) WC-3Ni, and (c) WC-7Ni*

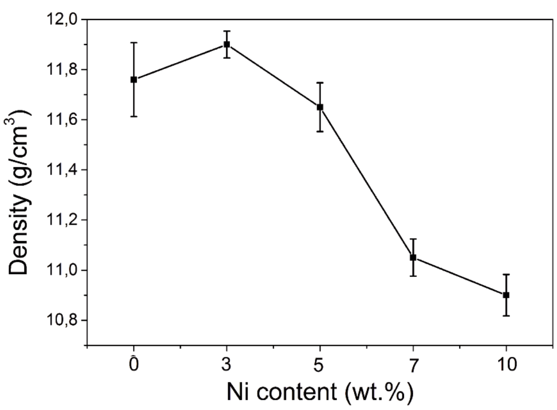


*Figure 3*. *Density of the infiltrated copper alloy matrix composites as a function of Ni content*

between copper alloy and the WC particles [48, 49]. In general, the spontaneous infiltration is mainly governed by the capillary forces. These later acts to pull the liquid copper alloy through the skeleton of WC particle. Whereas, these forces are mainly dependent on the wettability of molten liquid on the reinforcement surfaces of the particles [50]. Akhtar et al. [51] added alloying elements such as Ti, Al, Co, and Ni to the copper matrix in order to increase the wettability of the matrix phase with the reinforcements phase during liquid phase sintering. Moreover, it has been reported that the spreading of Ni on the WC particle interfaces can occur during solid-state sintering. Therefore, a continuous layer is formed on the WC particle surfaces when Ni wet and spread in this state. As a result, the wettability of the molten matrix on the reinforcement particle surfaces is improved. This enhances the densification of the composites [28, 48, 49]. However, increasing the Ni amount leads to a decrease in the reinforcement phase (WC particles) fraction, which increases the matrix phase fraction. Therefore, the density of the composites decreases.

### *3.3 Microstructural quantification*

Figure 4 presents SEM micrographs of the infiltrated composite reinforced with WC particles and its binary image. The binary image allows to separate the microstructure into two phases: the WC particles phase (white color) and the matrix phase (black color). Table 2 shows the mean values of the measured microstructure parameters for all the infiltrated composites using image analysis, including the particle size, the area fraction of the reinforcement phase, the binder mean free path and the porosity. Since no change was observed in the WC particles after infiltration (see Figures 2 (a-c)), the WC particles conserve their original shape. Therefore, the mean particle size was very similar for all the infiltrated composites.

Figures 5 and 6 show the particle size distribution and relative particle size distribution of the

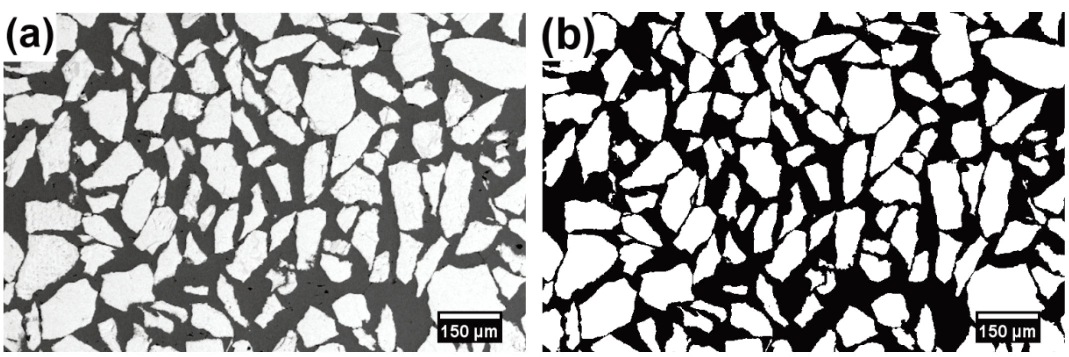


*Figure 4*. *SEM micrographs of the copper alloy matrix composites reinforced with WC particles: (a) original image and (b) binary image*

***Table 2.*** *Summarize of the microstructural parameters of the copper alloy matrix composites reinforced with WC-xNi powders*

| Parameters | WC | WC-3Ni | WC-5Ni | WC-7Ni | WC-10Ni |
|---|---|---|---|---|---|
| Particle size (µm) | 62.19 | 62.25 | 62.13 | 62.98 | 62.43 |
| Area fraction of WC particles (%) | 55.18 | 55.69 | 54.25 | 53.87 | 52.66 |
| Binder mean free path (µm) | 45.89 | 38.33 | 39.92 | 41.28 | 47.4 |
| Porosity (%) | 1.01 | 0.26 | 0.33 | 0.45 | 0.82 |

composites, which can be well fitted by a Weibull distribution. The Weibull distribution has the following cumulative density function:

$$F(G) = 1 - exp\left[-\left(\frac{G}{\eta}\right)\right]^{\beta} \quad (1)$$

Where G is the particle size, $\beta$ is the shape parameter (slope), which represents the covariance of the particle size data, and $\eta$ is the scale parameter, which represents the mean particle size. It can be seen that the Weibull distribution is in good agreement with all the measured particle size distributions of the infiltrated composites. However, it is found that it works better for the highest Ni addition. It has been reported that the sintered materials are well fitted with Weibull distribution [39, 52-55].

The WC particles area fraction results show that the addition of a small amount of Ni leads to an increase in the WC particle area fraction. However, increasing the Ni content above 5 wt.% leads to a decrease in the WC particles area fraction. On the contrary, the binder mean free path and porosity is found to increase with the increase of Ni content above 5 wt.%. The higher WC area fraction, the lower binder mean free path and porosity. The addition of a small amount of Ni was beneficial to increase the wettability, which results in good densification. However, a higher addition of Ni leads to a decrease in the area fraction of WC particles and an increase in the area fraction of the matrix.

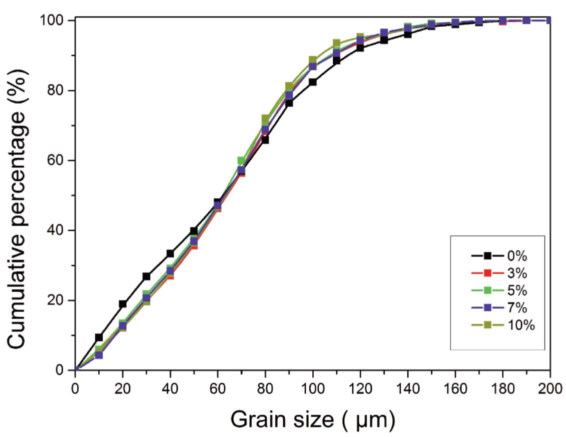


***Figure 5.*** *Cumulative distribution of particle size as a function of Ni content of the infiltrated copper alloy matrix composites reinforced with WC-xNi powders*

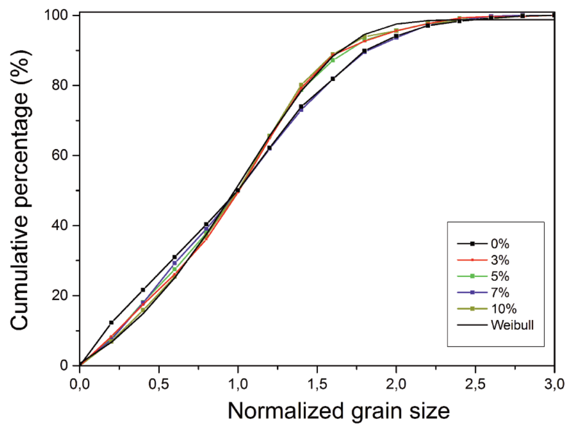


***Figure 6.*** *Relative particle size distributions of the copper alloy matrix composites reinforced with WC particles as a function of Ni content (0–10 wt.%) fitted by the Weibull distribution*

### *3.4 Effect of gravity*

Table 3 presents the area fraction of WC particles measured at three levels (bottom, middle and top) of each composite. It can be seen that the bottom level exhibits the highest WC area fraction in all the composites. During the infiltration process, the molten liquid is flowing into pores within the preform under the capillary forces. Due to the gravity effect and because of the large difference in density, WC particles can migrate towards and settle at the bottom of the composites. It has been reported that for liquid phase state systems, the segregation of particles occurs due to different parameters like density differences between the reinforced particles and the

***Table 3.*** *Area fraction of WC particles at different vertical positions in the infiltrated composites as a function of Ni content*

| Ni content (wt.%) | Area fraction of WC particles (%) | | | |
|---|---|---|---|---|
| | Bottom | Middle | Top | Mean |
| 0 | 56.63 | 55.16 | 53.75 | 55.18 |
| 3 | 56.66 | 56.11 | 54.29 | 55.69 |
| 5 | 55.54 | 53.78 | 53.43 | 54.25 |
| 7 | 55.37 | 54.79 | 51.44 | 53.87 |
| 10 | 53.78 | 53.09 | 51.1 | 52.66 |

matrix, the gravity forces, the viscosity of the molten, the packing porosity, interaction at the interface matrix/reinforcement, and solidification time [23, 56-59]. However, the segregation is found to be lower for the addition of a small amount of Ni (3 and 5 wt.%), which can be explained by the fact that when Ni wet and spread at solid state, a rigid WC skeletal can be formed. At the same time, a continuous layer is formed on the WC particles surface [28, 48, 49]. The continuous layer enhances the wettability of the molten matrix on the reinforcement particles surface. Therefore, the solid skeletal structure rigidity restricts the deformation after the inflow of the molten matrix. Similar results were observed when the W particles are coated with Cu to produce a W-Cu composite [60].

### *3.5 Pore size and distribution*

Figure 7 presents an optical image of the infiltrated composites reinforced with WC particles without the addition of Ni and the binary image of the detected pores. It can be seen that pores are frequently situated at the WC particles/matrix interfaces. The porosity results are given in Table 2. The porosity measurements indicate that the higher porosity is obtained for the composites reinforced with WC particles without the addition of Ni. Conversely, the addition of Ni can decrease the porosity of the composites. The lower porosity is found for the composites with a Ni addition of 3 wt.% and then increases with further addition. The pore formation during the infiltration process may result for different reasons, such as the poor wettability between the molten matrix and the reinforcement, the entrapped gases, or the differential shrinkage caused by the thermal expansion coefficient difference of the matrix and the reinforcement phase [61]. Lee et al. [62] reported that the poor wettability between the reinforcement and the matrix is one of the main reasons behind the porosity. Therefore, it is evident that the reduction in porosity is likely to be due to the enhancement of wettability between the WC particles and copper alloy by Ni addition. In addition, it has been reported that the addition in excess of the amount needed of the alloying elements leads to increase the viscosity of the molten matrix successively. Consequently, the infiltration rates decreases [49, 63], and leads to an increase in the porosity for the high Ni addition.

Figure 8 presents the pore size distribution of the infiltrated composites reinforced with WC particles as a function of Ni content. As can be seen, a high frequency of pores smaller than 8 μm is observed in all composites. In addition, the number of pores is higher for the composites without Ni addition compared to the other composites. It is well known that for the infiltration process, capillary forces drive molten liquid to wet the pores, which are

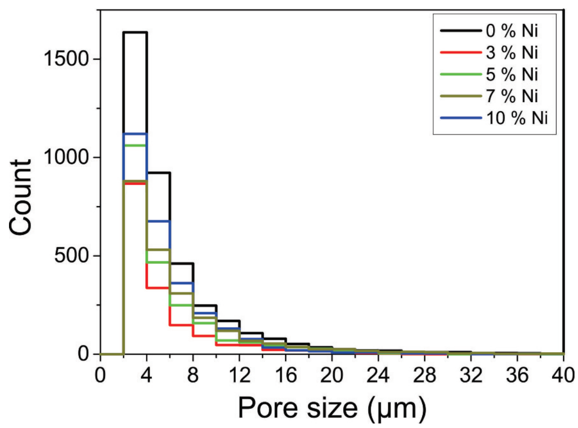


***Figure 8**. Pore size distribution in the infiltrated copper alloy matrix composites reinforced with WC particles as a function of Ni content*

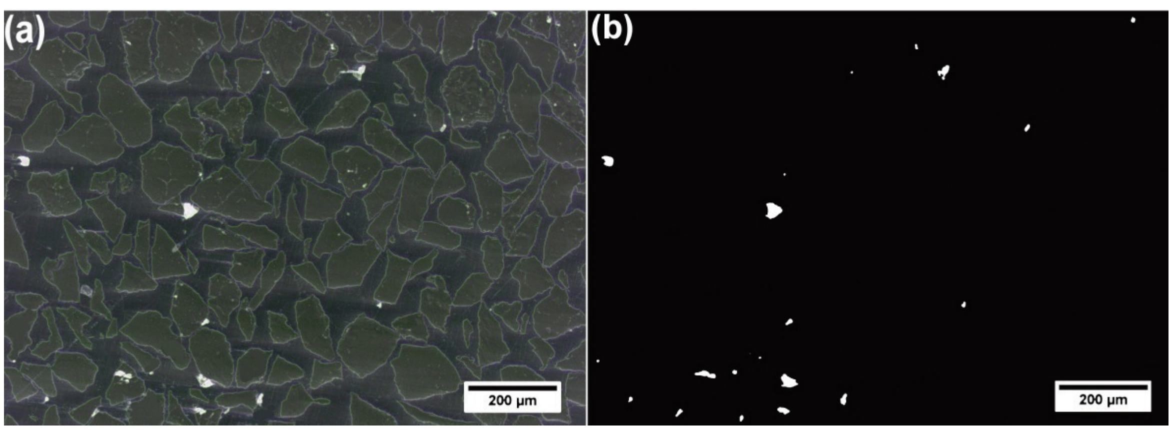


***Figure 7**. Optical image of the infiltrated copper alloy matrix composite reinforced with WC particles and the binary image of the pores: (a) original image and (b) binary image*

collected between the particles. Further, the capillary forces are proportionally related to the wettability. At the same time, the molten liquid preferentially fills the smaller pores. As a result, the amount of pores decreases for the composites with Ni addition [64].

### *3.6 Hardness*

Figure 9 shows the hardness of the infiltrated composites as a function of Ni content. It can be seen that the hardness of the composites reinforced with WC and WC-*x*Ni (276-327 HV) are higher than that of the copper alloy used as the matrix (154 ± 4 HV). The increase in hardness is due to the reinforcement particles strengthening effect on the metal matrix [9, 46]. WC particles improve the hardness of the composites by stopping the dislocation motion at reinforcement/matrix interface [65]. Moreover, the hardness is observed to follow the same trend as the density. The dependent relation between the hardness and the density was reported in several studies [66-68], the higher density of the composites is, the higher the hardness becomes. Note that the hardness slightly increases for the composite with a small addition of Ni (3 wt.%). As the Ni content increases, the hardness of the composites is substantially reduced. It seems that this decrease in hardness is attributed to the increase in ductile phase content. Sanchez et al.[69] concluded from their study that the hardness of the composite prepared with the centrifugal infiltration process depends on the volume fraction of the reinforcement. Similar results have also been reported in different studies [33, 70, 71]. From these findings, it can be inferred that the density and hardness results are in good agreement with the microstructural quantification results (area fraction and binder mean free path presented in Table 2).

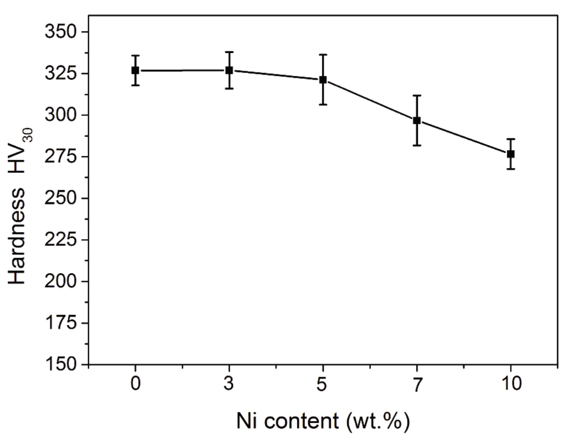


***Figure 9***. *Hardness of the infiltrated copper alloy matrix composites as a function of Ni content*

## 4. Conclusions

Copper alloy matrix composites reinforced with WC particles with the addition of different Ni contents were prepared by the spontaneous infiltration process. Image analysis technique was used to quantify the different microstructural parameters to investigate the effect of Ni addition. The infiltrated composites present a uniform distribution of the reinforcement in the matrix. It was found that small addition of Ni (3 wt.%) improves the densification, density and hardness results of the infiltrated composites. However, the increase of Ni content above this value leads to decrease the microstructural features and composites properties. These results are mainly related to the enhancement of the wettability between the molten matrix and the reinforcement particles. No change or dissolution is observed on the WC particles. Microstructural quantification indicates that the Weibull distribution is found to fit the particles size for the infiltrated composites. The porosity results also show a significant decrease with Ni addition. The density and hardness results are in good agreement with the quantified microstructural parameters.

## Acknowledgement

*The financial and technical support of the Laboratory of Science and Materials Engineering (LSGM), University of Science and Technology Houari Boumediene Algeria (USTHB), the Scientific Research Project Unit of Kocaeli University, Turkey, and the production tools division of (ENSP) company Algeria are greatly acknowledged.*

## References

[1] A. Mortensen and J. Llorca, Annu. Rev. Mater. Res, 40 (2010) 243-270.

[2] B. Cantor, F. P. Dunne, and I. C. Stone, Metal and ceramic matrix composites, CRC Press, 2003.

[3] I. Chang and Y. Zhao, Advances in Powder Metallurgy: Properties, Processing and Applications, Elsevier, 2013.

[4] T. Clyne, An introductory overview of MMC systems, types, and developments, Comprehensive composite materials, Elsevier, 2000, 1-26.

[5] S. Suresh, Fundamentals of metal-matrix composites, Elsevier, 2013.

[6] N. Natarajan, V. Krishnaraj, and J. P. Davim, Metal matrix composites: synthesis, wear characteristics, machinability study of MMC brake drum, Springer, 2014.

[7] M. Reyes and A. Neville, Wear, 255 (2003) 1143-1156.

[8] K. Kembaiyan and K. Keshavan, Wear, 186 (1995) 487-492.

[9] E. Hong, B. Kaplin, T. You, M.-s. Suh, Y.-S. Kim, and H. Choe, Wear, 270(9) (2011) 591-597.
[10] P. Deshpande and R. Lin, Mater. Sci. Eng., A, 418(1) (2006) 137-145.
[11] M. Yusoff, R. Othman, and Z. Hussain, Mater. Desi., 32(6) (2011) 3293-3298.
[12] J. Liu, S. Yang, W. Xia, X. Jiang, and C. Gui, J. Alloy. Compd., 654 (2016) 63-70.
[13] Y. Sun, H. Wu, M. Li, Q. Meng, K. Gao, X. Lü and B. Liu, Materials, 5 (2016) 343.
[14] S. Tan, X. Fang, K. Yang and L. Duan, Int. J. Refract. Metals. Hard. Mater., 43 (2014) 186-92.
[15] M. Li, Y. Sun, B. Dong, H. Wu and K. Gao, Mater. Res. Innov., no. sup5 (2015) S5-59-S5-63.
[16] L. J. de Oliveira, S. C. Cabral and M. Filgueira,Int. J. Refract. Metals. Hard. Mater., 35 (2012) 228-34.
[17] W. Li, J. Zhan, S. Wang, H. Dong, Y. Li and Y. Liu, Rare Metals,31(1) (2012): 81-87.
[18] C.-Y. Chung, M.-T. Lee, M.-Y. Tsai, C.-H. Chu and S.-J. Lin, Appl. Therm. Eng., 69(1) (2014) 208-13.
[19] C. Zhao, J. U. Pet. China Nat. Sci. E., 20 (1996) 65-69.
[20] Y.-m. Fan, H. Guo, J. Xu, K. Chu, X.-x. Zhu and C.-c. Jia, Int. J. Min. Met. Mater., 18(4) (2011) 472.
[21] M. Li, Y. Sun, Q. Meng, H. Wu, K. Gao and B. Liu, Materials, 9(12) (2016): 1006.
[22] V. Michaud and A. Mortensen, Composites Part A, 32 (2001) 981-996.
[23] A. Mortensen, Melt infiltration of metal matrix composites, Comprehensive composite materials, Elsevier, 2000, 521-554.
[24] N. Eustathopoulos, A. Mortensen, and S. Suresh, Capillary phenomena, interfacial bonding and reactivity, Butterworths,1993.
[25] J. Fridlyander, Metal matrix composites, Springer Science & Business Media, 2012.
[26] A. Léger, L. Weber, and A. Mortensen, J. Mater. Sci., 49 (2014) 7669-7678.
[27] V. Silva, C. Fernandes, and A. Senos, Ceram. Int., 42(1) (2016) 1191-1196.
[28] H. De Macedo, A. Da Silva, and D. de Melo, Mater. Lett., 57(24) (2003) 3924-3932.
[29] O. M. Alzouma, M.-A. Azman, D.-L. Yung, V. Fridrici, and P. Kapsa, Wear, 352 (2016) 130-135.
[30] Y. Xu, Z. Yang, Z. Han, G. Liu, and J. Li, Ceram. Int., 40(1) (2014) 1037-1043.
[31] N. Lin, Y. Jiang, D. Zhang, C. Wu, Y. He, and D. Xiao, Int. J. Refract. Metals. Hard. Mater., 29(4) (2011) 509-515.
[32] K. Eun, D. Kim, and D. Yoon, Powder Metall., 27(2) (1984) 112-114.
[33] X. Zhang, J. Zhou, N. Lin, K. Li, K. Fu, B. Huang, and Y. He, Int. J. Refract. Metals. Hard. Mater., 57 (2016) 64-69.
[34] L. Wojnar, Image analysis: applications in materials engineering, Crc Press, 1998.
[35] Wojnar, Leszek, Krzysztof J. Kurzydlowski, and Janusz Szala. Mater. Park., OH: ASM Inter., (2004) 403-427.
[36] J. J. Friel, Practical guide to image analysis, ASM international, 2000.
[37] M. Charpentier, A. Hazotte, and D. Daloz, Mater. Sci. Eng., A, 491(1) (2008) 321-330.
[38] H. E. Exner, Image Anal. Stereol., 23(2) (2011) 73-82.
[39] J. Shen, L. Campbell, P. Suri, and R. M. German, Int. J. Refract. Metals. Hard. Mater., 23 (2005) 99-108.
[40] A. Petersson and J. Ågren, Acta Mater., 53 (2005) 1673–1683.
[41] O. Dengiz, R. McAfee, I. Nettleship, and A. E. Smith, J. Eur. Ceram. Soc., 27 (2007) 1927-1933.
[42] A. M. Gokhale, Microsc. Microanal., 22 (2016) 1966-1967.
[43] M. Coster, X. Arnould, J. Chermant, L. Chermant, and T. Chartier, J. Eur. Ceram. Soc., 25 (2005) 3427-3435.
[44] Anon, Standard Test Methods for Density of Compacted or Sintered Powder Metallurgy (PM) Products Using Archimedes’ Principle. 2008, ASTM International.
[45] Anon, Standard Test Methods for Vickers Hardness and Knoop Hardness of Metallic Materials. 2017, ASTM International.
[46] P. Deshpande, J. Li, and R. Lin, Mater. Sci. Eng., A, 429(1) (2006) 58-65.
[47] J. L. Johnson and R. M. German, Metall. Mater. Trans. B, 27 (1996) 901-09.
[48] J. M. Missiaen, Mater. Sci. Eng., A, 475 (2008) 2-11.
[49] T.-H. Ihn, S.-W. Lee and S.-K. Joo, Powder Metall., 37 (1994) 283-88.
[50] P. Ho, Q. Li and J. Fuh, Mater. Sci. Eng., A, 485 (2008) 657-63.
[51] F. Akhtar, S. J. Askari, K. A. Shah, X. Du, and S. Guo, Mater. Charact., 60(4) (2009) 327-336.
[52] German, R. M., Crit. Rev. Solid State Mater. Sci., 35(4) (2010) 263-305.
[53] Johnson, J. L.; Campbell, L. G.; Park, S. J.; German, R. M, Metall. Mater. Trans. A,40.2 (2009) 426.
[54] Liu, Y.; German, R.; Iacocca, R., Acta. Mater., 47 (3) (1999) 915-926.
[55] Fang, Z.; Patterson, B. R.; Turner, M. E., Mater. Charact., 31 (3) (1993) 177-182.
[56] Panda, E.; Mehrotra, S.; Mazumdar, D., Metall. Mater. Trans. A,37 (5) (2006) 1675-1687.
[57] Tewari, A.; Gokhale, A.; German, R., Acta. Mater., 1999, 47, (13), 3721-3734., 47 (13) (1999) 3721-3734.
[58] Kipphut, C.; Bose, A.; Farooq, S.; German, R., Metall. Mater. Trans. A, 19 (8) (1988) 1905-1913.
[59] German, R. M., Fund.Refract. Technol., (2001) 3-28.
[60] A. Ibrahim, M. Abdallah, S. Mostafa and A. A. Hegazy, Mater. Desi., 30(4) (2009) 1398-1403.
[61] S. Ren, X. He, X. Qu, and Y. Li, J. Alloy. Compd., 455 (2008) 424-431.
[62] H. Lee and S. Hong, Mater. Sci.Tech., 19 (2003) 1057-64.
[63] D. Manfredi, M. Pavese, S. Biamino, A. Antonini, P. Fino and C. Badini, Composites Part A, 41 (2010) 639-45.
[64] R. M. German, P. Suri and S. J. Park, J. Mater. Sci.,44 (2009) 1-39.
[65] K.-C. Zhou, H.-L. Pei, J.-K. Xiao and L. Zhang, Rare

Metals,1-6.

[66] J. Johnson and R. German, Metall. Mater. Trans. A, 24 (1993) 2369-77.

[67] H. Abbaszadeh, A. Masoudi, H. Safabinesh and M. Takestani, Int. J. Refract. Metals. Hard. Mater., 30 (2012) 145-51.

[68] H. Ibrahim, A. Aziz and A. Rahmat, Int. J. Refract. Metals. Hard. Mater., 43 (2014) 222-26.

[69] M. Sánchez, J. Rams and A. Ureña, Composites Part A,41 (2010) 1605-11.

[70] H.-C. Kim, I.-J. Shon, J.-K. Yoon, J.-M. Doh, and Z. A. Munir, Int. J. Refract. Metals. Hard. Mater., 24(6) (2006) 427-431.

[71] N. Ray, B. Kempf, T. Mützel, F. Heringhaus, L. Froyen, K. Vanmeensel, and J. Vleugels, J. Alloy. Compd., 670 (2016) 188-197.

# KARAKTERIZACIJA MIKROSTRUKTURE I KVANTITATIVNA ANALIZA MATRIČNOG KOMPOZITA LEGURE BAKRA, OJAČANOG WC-*x*Ni PRAHOM, KOJI JE DOBIJEN POSTUPKOM SPONTANE INFILTRACIJE

**I. Daoud [a], Dj. Miroud [a], R. Yamanoglu [b*]**

[a] Univerzitet nauke i tehnologije HOUARI BOUMEDIENE, Laboratorija za nauku i inženjerstvo materijala, Alžir, Alžir

[b] Kocelji univerzitet Odsek za metalurgiju i inženjerstvo materijala, Izmit, Turska

***Apstrakt***

*Tokom ovog istraživanja, postupkom spontane infiltracije, dobijeni su matrični kompoziti legure bakra ojačani česticama volfram-karbida uz dodavanje različitog sadržaja Ni (0, 3, 5, 7 i 10 wt%). Postupak analize slika korišćen je za određivanje mikrostrukturnih parametara, kao što su veličina čestice i njihova distribucija, površina loma, srednji slobodni put vezivnog metala, kao i veličina pora. Ispitivan je i uticaj dodavanja Ni na mikrostrukturu, gustinu i tvrdoću. Dobijeni rezultati pokazuju da dodavanje male količine Ni poboljšava proces učvršćivanja ubačenih kompozita. Najveće vrednosti za gustinu, 11.84 g/cm$^3$, i tvrdoću, 327HV, dobijene su za kompozit sa dodatkom 3wt.% Ni. Rezultati kvantitativne analize se slažu sa dobijenim podacima o osobinama mikrostrukture i dobijenim vrednostima za tvrdoću.*

**Ključne reči:** *Metalni matrični kompoziti; Čestice volfram-karbida; Analiza slike; Kvantifikacija; Mikrostruktura*